Soil-structure interface resistance changes due to rigid awns

Ryan D. Beemer, Ph.D., ¹ Joe Tom, PhD, ^{2,3} Kaylee Tucker, ⁴ Ann C. Sychterz, PhD, ⁵ and Isabella Bernardi⁶

¹Department of Civil and Environmental Engineering, University of Massachusetts Dartmouth, 285 Old Westport Rd, North Dartmouth, MA 02747; E-mail: rbeemer@umassd.edu

²University of Illinois Urbana-Champaign, Department of Civil and Environmental Engineering, Urbana, Illinois, 61801; E-mail: <u>joetom@illinois.edu</u>

3U.S. Army Engineer Research and Development Center, 3909 Halls Ferry Rd., Vicksburg, MS 39180, Email: Joe.G.Tom@erdc.dren.mil

⁴University of Illinois Urbana-Champaign, Department of Civil and Environmental Engineering, Urbana, Illinois, 61801; E-mail: katucke2@illinois.edu

⁵University of Illinois Urbana-Champaign, Department of Civil and Environmental Engineering, Urbana, Illinois, 61801; E-mail: asychter@illinois.edu

⁶GZA, 188 Valley Street Suite 300, Providence, RI 02909; E-mail: Isabella.bernardi@gza.com

ABSTRACT

This paper presents a study on the impact of rigid awns and their deployment on interface friction. Awns are appendages attached to the exterior surface of a geo-system and bio inspired by grass seeds. Awns provide frictional anisotropy and assist the seed in self-embedding into the soil or clinging to animal hair. In geo-systems, like piles, deployable awns can provide frictional anisotropy reducing installation effort and increasing global capacity. In addition, flexible awns can be folded up to enable space saving for transportation. This paper presents the results from a set of interface shear tests in a modified direct shear device. Single rigid awns were tested at various angles, from horizontal, as a pseudo-static simulation of deployment, in loose and dense sand, in both the cranial (towards the head) and caudal (towards the tail direction). It is shown that awns opened at larger angles provide higher interface friction and that shearing in the cranial direction provided more resistance than in the caudal direction. This demonstrates that deployable awns could be used in geosystems to provide friction anisotropy and increase capacity.

INTRODUCTION

A key feature of deployable structures is that they change shape to change size. These structures deploy by expanding in shape when their size is increased (Pellegrino 2001). Deployable and compliant structures have potential within the field of civil engineering thanks to their potential for increased capacity and decreased embodied energy. Two common applications of deployable

structures take advantage of these features. For temporary installments—like emergency shelters (Cai et al. 2015)—lightweight, movable, and easy to erect structures are required. Larger scale systems (García-Mora and Sánchez-Sánchez 2021) and space structures, such as masts, solar arrays, and antennae (Furuya 1992; G. Tibert 2002), are designed to be lightweight and compact for ease of transportation (Gantes et al. 1989). In practice, many contemporary structures use preconnected parts for easier deployment. Locking mechanisms may also be necessary for deployable structures that are stress-free before, during, and after deployment (A. G. Tibert and Pellegrino 2003). Construction of deployable structures has focused on these aboveground structures but has not yet been expanded to underground use.

Compliant structures are similar to deployable structures in that they change shape. However, instead of changing shape by changing size, compliant structures change shape through elastic or plastic material deformation. Compliant elements are singular elements that deform to perform their functions (Howell et al. 2013). These biologically inspired mechanisms function without joints and, like natural elements, are flexible (Kota et al. 2001). Compliant structures also have advantages in assembly and manufacturing because as singular elements, there is little assembly or pre-connection required (Zentner and Böhm 2009). While new work has been done to scale up compliant structures to the building scale for use in façades (Schleicher 2015), compliant structures tend to be used in small scale applications such as microelectromechanical systems (Poppinga et al. 2016).

Although most geotechnical engineering systems do not change shape, this is beginning to change within the area of pile-based anchors (Giampa et al. 2017; Wilde et al. 2001). Existing work has been done regarding underground geostructures that involve fins. Static radial fins on buried pipelines were found to better resist uplift loads when installed in sand and varied with fin configuration and geometry (Tom et al. 2017). Piles that have anchor wings have also been explored. After a pile is rotated into sand, wings hinge outward into sand and provide improved resistance to uplift loads (Sakr et al. 2023). In addition, static piles with snakeskin inspired geometries have been tested (O'Hara and Martinez 2020). While these studies have explored the advantages of deployability or biological inspiration, they either have no motion involved or work through rigid body motion. Compliant and deployable systems, which change shape and size elastically, have not yet been explored within geotechnical engineering.

The shear and load transfer behavior of soil-structure interfaces is a key factor in the ability of underground structures to resist global loading and prevent geotechnical failure, either via compression or tension. Tension-loaded axial piles, for instance, are an example of a geotechnical structure that derives the majority of its geotechnical capacity from the soil-structure interface response (Fleming et al. 2008). Significant recent research has explored the idea of adding various external elements or features structural interfaces to study surface roughness and to enhance the load-carrying capacity (Frost and DeJong 2005; Martinez et al. 2019; O'Hara and Martinez 2020; Stutz et al. 2019). These novel ideas in particular derive inspiration from nature, primarily in the form of the asymmetric profile of snake scale, to generate anisotropic interface responses, where the resistance is larger in one direction than the other. These studies focused on inclusion of

surficial roughness variations on the order of 1-10 grain diameters for the sandy materials tested. These variations were sufficient to create increases in tangential friction enabling a smooth metal interface to become approximately equivalent to a fully rough interface (O'Hara and Martinez 2020), while maintaining directional asymmetry when loaded in opposite direction. In practice, these snake-skin inspired interfaces provide the potential (in the case of piles) to reduce installation requirements while increasing the resistance when the structure is subsequently loaded in the opposing direction. The added benefit of these types of interface modifications is potentially more accurately estimates of interface friction, since the resistances appear to generally trend toward the fully rough condition, with the exception of (Stutz et al. 2021) who recently demonstrated resistances larger than fully rough through the inclusion of multiple structural extrusions into a sandy sample in direct shear testing. Although increases in interface friction appear are well documented, there remain opportunities to further enhance these gains through other sources of bio-inspiration. This study focuses on external appendages (or "awns") on cheat grass seeds. They point primarily in one direction and exhibit compliance to ease penetration into animal fur, for dispersal, or soil, for propagation, (Elbaum et al. 2007; Morrow and Stahlman 1984).

EXPERIMENTAL APPARATUS

Awn shear tests were conducted using a GeoComp Shear Trac-II. A custom shear box was created to allow for 3-D printed awn to be inserted into the baseplate, Figure 1. To enable placement of awns, the shearbox baseplate was constructed from aluminum with a small slot in the center, which extended the width of the carriage with gaps of approximately 1 mm on each end. Swappable awns could be placed into the slots, with portions remaining in the soil containment area, and bolted into place from the back. Awns were 3D printed from combinations of VeroYellow-V plastic (yield strength of 65 MPa) and Agilus photopolymer (yield strength 2.5 MPa). Rigid awns were comprised of 100% plastic, and flexible awns were comprised of 95% plastic and 5% Agilus. Figure 2 shows a schematic of typical awn dimensions and geometrical properties, including the awn angle, α.

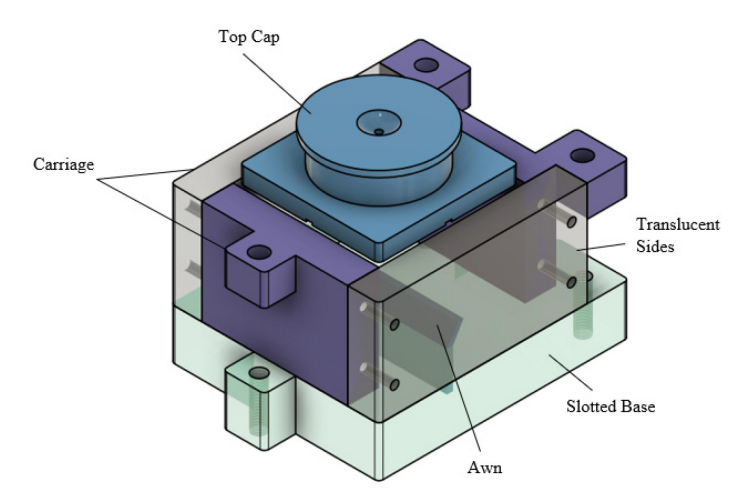


Figure 1. Three-Dimensional Model of Shear Box with Awn

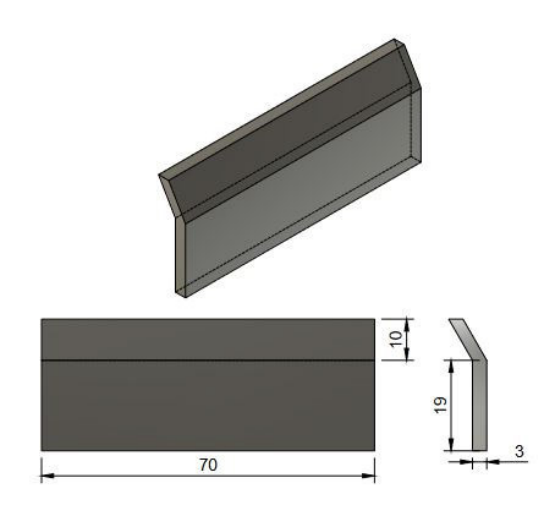


Figure 2. Three-Dimensional Model of Rigid Awn

SOIL USED IN THE EXPERIMENT

The experiments used the commercially produced Ottawa F-65 sand, which is a poorly graded silica sand with a median grain size of approximately, $D_{50} = 0.2$ mm (El Ghoraiby et al. 2020). Engineering properties of Ottawa F-65 are listed in Table 1. Samples were prepared at two relative densities, D_R , 20% and 80%. Loose ($D_R = 20\%$) samples were prepared via air pluviation through a funnel in three lifts. Dense ($D_R = 80\%$) samples were prepared via air pluviation, but each lift was tamped following placement. The awn did limit the ability to tamp the sample uniformly and as a result relative density varied by $\pm 10\%$ between samples. Vertical strain was measured during testing to verify correct volumetric behavior and results were analyzed to 5% horizontal normalized displacement to minimize the impact of relative density variation.

Table 1. Ottawa F-65 Properties as per (El Ghoraiby et al. 2020)

| Property | Value | |
|--|--------|--|
| Specific Gravity, G_s | 2.65 | |
| Median Particle Diameter, <i>D</i> ₅₀ | 0.2 mm | |
| Coefficient of Uniformity, C_u | 1.7 | |
| Coefficient of Curvature, C_c | 1.0 | |
| Maximum Void Ratio, <i>e</i> _{max} | 0.83 | |
| Minimum Void Ratio, e_{min} | 0.51 | |

EXPERIMENTS

To study the impact a compliant awn opening during interface shearing, awn deployment was mimicked by varying the angle of rigid awns in the experiment from $\alpha = 10$ -60°. A total of 22 interface shear tests with a rigid awn were completed using the Shear Trac-II and presented in this study, but additional tests and analyses are presented in Bernardi (2022). Directional anisotropy was investigated by shearing independently in both the cranial direction (towards the head) and caudal direction (towards the tail), illustrated in Figure 3 where the arrow represents the relative movement of sand. Samples were prepared at 20% and 80% relative density to assess their effects. A testing matrix summarizing of all trials is described in Table 2.



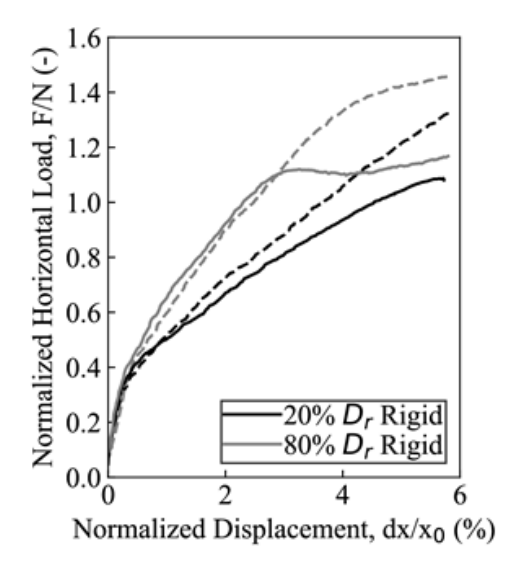
Figure 3. Representation of directional anisotropy terminology

RESULTS AND DISSCUSION

The load displacement behavior of an example interface shear test with an awn at a 40° angle is presented in Figure 4; additional tests are available in Bernardi (2022). When sheared in the cranial direction the normalized interface friction more or less exhibited a strain hardening behavior, Figure 4a. The rate of hardening decreased around 4% normalized displacement. In the caudal direction most tests exhibited a peak strength somewhere between 2% - 3% normalized displacement, Figure 4a. Measured vertical deformations matches correlates to the relative density of the sand. Regardless of awn orientation the loose, $D_R = 20\%$ samples all contracted and the dense, $D_R = 80\%$ samples all dilated, Figure 4b. This indicates that the presence of the awn and boundary effects did not override typical soil behavior.

Table 2. Experimental Testing Matrix

| Cranial Direction | | Caudal Direction | |
|-------------------|-------------------------|---------------------|-------------------------|
| Awn Angle, α | Relative Density, D_R | Awn Angle, α | Relative Density, D_R |
| (°) | (%) | (°) | (%) |
| 60 | 80 | 60 | |
| 50 | | 50 | |
| 40 | | 40 | 90 |
| 30 | | 30 | 80 |
| 20 | | 20 | |
| 10 | | 10 | |
| 60 | 20 | 60 | |
| 50 | | 50 | |
| 40 | | 40 | 20 |
| 30 | | 30 | 20 |
| 20 | | 20 | |
| 10 | | 10 | |



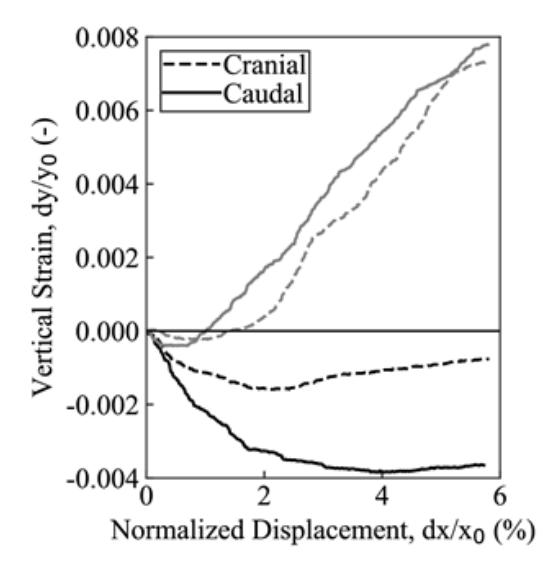


Figure 4. Example interface resistance behavior with rigid awn at 40° (note legends in both subfigures). Normalized horizontal load versus normalized displacement (left). Vertical strain versus normalized displacement (right).

The impact of awn angle on normalized horizontal force is presented in Figure 5, in respect to the magnitude of normalized displacement of 1%, 2%, 3%, 4%, and 5%. In all cases, normalized horizontal load increased with awn angle up to awn angles $\alpha \sim 40^{\circ}$ - 50°. In most tests the normalized load decreased between awn angle $\alpha \sim 40^{\circ}$ - 50° and $\alpha = 60^{\circ}$. Interestingly, the slope or rate of normalized load on awn angle increased with larger normalized displacements. At large normalized displacements of 5% opening the awn angle from 10° to 40° when shearing in the

cranial direction increased the normalized load by about 25%, Figure 5a. This a appears to be larger than the increase due to switching from the caudal to cranial direction at the same awn angle; in particular for the samples tested at a relative density of 20%. This is substantially less than what was predicted by finite element numerical models. Bernardi (2022) and Sychterz et al. (2021) showed a 350% increase in load between 10° and 40°. This could be due to the awns not being perfectly rigid as they were in the finite element models or the difference in boundary conditions between the model and the experiments; further study is needed.

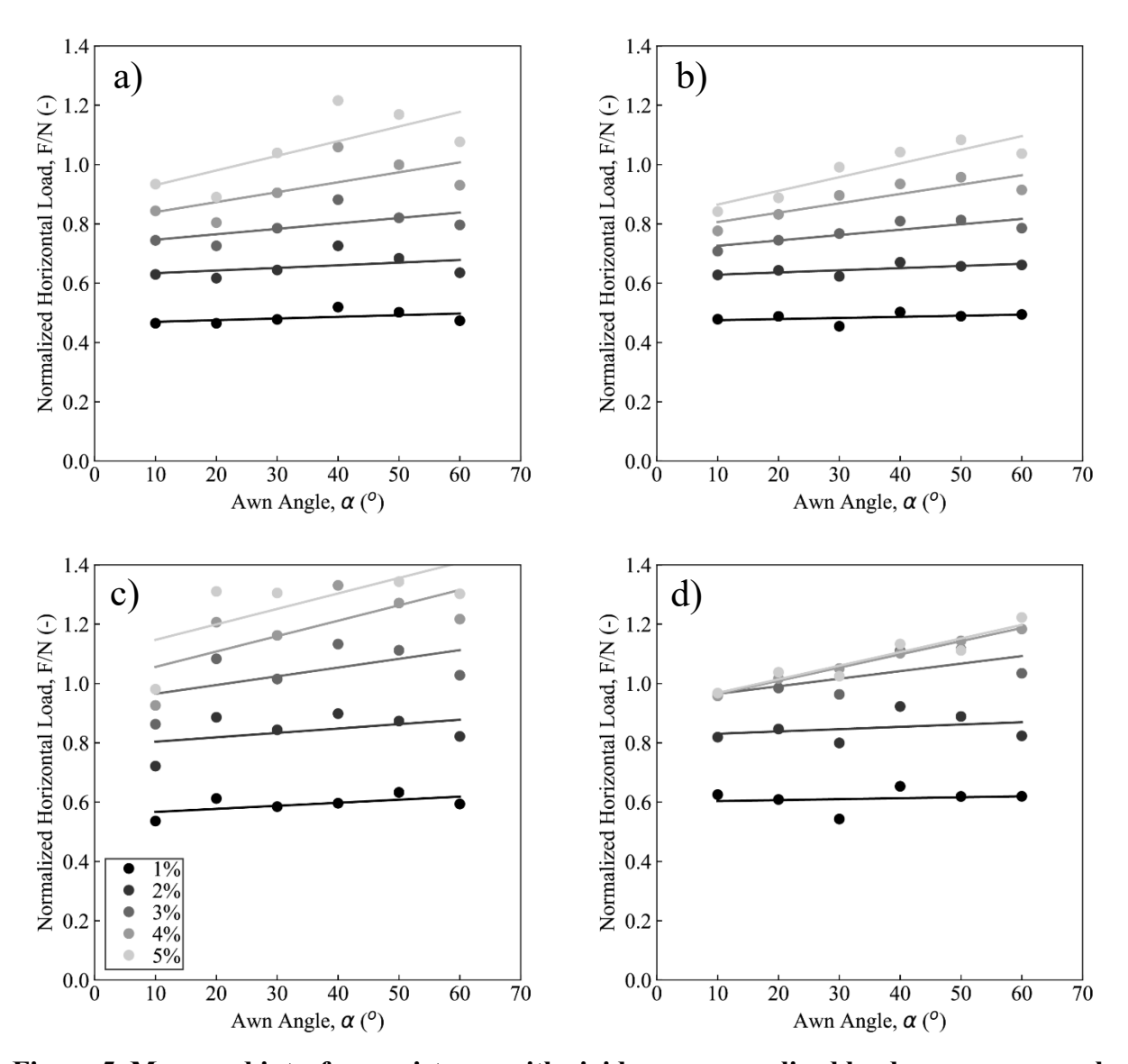


Figure 5. Measured interface resistance with rigid awn, normalized load versus awn angle for increasing values of normalized displacement. Lines represent linear best-fits to the data. a) Cranial direction and $D_R = 20\%$, b) Caudal direction and $D_R = 20\%$, c) Cranial direction and $D_R = 80\%$, d) Caudal direction and $D_R = 80\%$

In all tests denser samples exhibited higher normalized horizontal load which is expected given their dilative behavior. There appeared to be more variation in the measured normalized horizontal load for the dense samples than the loose samples, Figure 5a vs. Figure 5c and Figure 5b vs. Figure 5d. This is likely the result of sample preparation, as it was difficult to tamp around the awn and densify the soil so relative density varied by $\pm 10\%$. In all cases higher normalized horizontal load was measured when shearing in the cranial direction, however at large displacements increasing the awn angle, α , had a greater on the resistance.

CONCLUSION

From this study on the effects of rigid awns with different angular orientations on interface shearing and anisotropy the following conclusions can be drawn:

- Changing the orientation of the awn angle from 10° to 40° can increase the normalized horizontal load by approximately 25% at large displacements. This is significantly less than predicted in previous finite element studies, but still significant.
- Increasing awn angle, α , (i.e., representing a more deployed state) has a larger impact on measured normalized horizontal load at larger displacements. This indicates large deformations are likely needed to gain benefit from compliant geo-systems.
- Increasing the awn angle from 10° to 40° appears to have a larger impact on normalized load than directional anisotropy, that is shearing in the cranial versus caudal direction.
- The presence of the awn did not appear to significantly impact vertical strain behavior and as such, tests with dense sand had larger normalized horizontal forces than tests with loose sands.

REFERENCES

- Bernardi, I. J. 2022. "Study of Frictional Anisotropy on Bio-Inspired Soil-Structure Interfaces for Pile and Anchor System Applications." Thesis. Dartmouth, MA: University of Massachusetts Dartmouth.
- Cai, J., X. Deng, Y. Xu, and J. Feng. 2015. "Geometry and motion analysis of origami-based deployable shelter structures." *J. Struct. Eng.*, 141 (10): 06015001. American Society of Civil Engineers.
- El Ghoraiby, M., H. Park, and M. T. Manzari. 2020. "Physical and mechanical properties of Ottawa F65 sand." *Model Tests Numer. Simul. Liq. Lateral Spreading LEAP-UCD-2017*, 45–67. Springer.
- Elbaum, R., L. Zaltzman, I. Burgert, and P. Fratzl. 2007. "The Role of Wheat Awns in the Seed Dispersal Unit." *Science*, 316 (5826): 884–886. https://doi.org/10.1126/science.1140097.
- Fleming, K., A. Weltman, M. Randolph, and K. Elson. 2008. Piling engineering. CRC press.
- Frost, J. D., and J. T. DeJong. 2005. "In Situ Assessment of Role of Surface Roughness on Interface Response." *J. Geotech. Geoenvironmental Eng.*, 131 (4): 498–511. https://doi.org/10.1061/(ASCE)1090-0241(2005)131:4(498).

- García-Mora, C. J., and J. Sánchez-Sánchez. 2021. "The convergence surface method for the design of deployable scissor structures." *Autom. Constr.*, 122: 103488. Elsevier.
- Giampa, J. R., A. S. Bradshaw, and J. A. Schneider. 2017. "Influence of dilation angle on drained shallow circular anchor uplift capacity." *Int. J. Geomech.*, 17 (2): 04016056. American Society of Civil Engineers.
- Howell, L. L., S. P. Magleby, and B. M. Olsen. 2013. "Handbook of Compliant Mechanisms." *John Wiley Sons Ltd Hoboken*. Wiley Online Library.
- Kota, S., J. Joo, Z. Li, S. M. Rodgers, and J. Sniegowski. 2001. "Design of compliant mechanisms: applications to MEMS." *Analog Integr. Circuits Signal Process.*, 29: 7–15. Springer.
- Martinez, A., S. Palumbo, and B. D. Todd. 2019. "Bioinspiration for Anisotropic Load Transfer at Soil–Structure Interfaces." *J. Geotech. Geoenvironmental Eng.*, 145 (10): 04019074. https://doi.org/10.1061/(ASCE)GT.1943-5606.0002138.
- Morrow, L. A., and P. W. Stahlman. 1984. "The History and Distribution of Downy Brome (*Bromus tectorum*) in North America." *Weed Sci.*, 32 (S1): 2–6. https://doi.org/10.1017/S0043174500060173.
- O'Hara, K. B., and A. Martinez. 2020. "Monotonic and Cyclic Frictional Resistance Directionality in Snakeskin-Inspired Surfaces and Piles." *J. Geotech. Geoenvironmental Eng.*, 146 (11): 04020116. https://doi.org/10.1061/(ASCE)GT.1943-5606.0002368.
- Pellegrino, S. 2001. Deployable structures in engineering. Springer.
- Poppinga, S., A. Körner, R. Sachse, L. Born, A. Westermeier, L. Hesse, J. Knippers, M. Bischoff, G. T. Gresser, and T. Speck. 2016. "Compliant mechanisms in plants and architecture." *Biomim. Res. Archit. Build. Constr. Biol. Des. Integr. Struct.*, 169–193. Springer.
- Sakr, M., A. Nazir, W. Azzam, and I. GamalEldin. 2023. "Group efficiency of tension double under-reamed piles in sand." *Indian Geotech. J.*, 53 (1): 11–28. Springer.
- Schleicher, S. 2015. Bio-inspired compliant mechanisms for architectural design: transferring bending and folding principles of plant leaves to flexible kinetic structures.
- Stutz, H. H., A. Martinez, L. Heepe, H. Tram Tramsen, and S. N. Gorb. 2019. "Strength anisotropy at soil-structure interfaces with snake skin inspired structural surfaces." *E3S Web Conf.*, (A. Tarantino and E. Ibraim, eds.), 92: 13008. https://doi.org/10.1051/e3sconf/20199213008.
- Stutz, H., H. Tramsen, L. Heepe, and S. Gorb. 2021. "Strength and deformation behaviour of bio-inspired blade like surfaces sliding along a soil-structure interface." *ALERT Geomaterials*, 62.
- Sychterz, A., I. Bernardi, J. G. Tom, and R. D. Beemer. 2021. "Nonlinear soil-structure behavior of a deployable and compliant anchor system." *Can. J. Civ. Eng.*, cjce-2021-0204. https://doi.org/10.1139/cjce-2021-0204.
- Tom, J., C. O'loughlin, D. White, A. Haghighi, and A. Maconochie. 2017. "The effect of radial fins on the uplift resistance of buried pipelines." *Géotechnique Lett.*, 7 (1): 60–67. Thomas Telford Ltd.
- Wilde, B., H. Treu, and T. Fulton. 2001. "Field testing of suction embedded plate anchors." *Elev. Int. Offshore Polar Eng. Conf.* OnePetro.
- Zentner, L., and V. Böhm. 2009. "On the classification of compliant mechanisms." *Proc. EUCOMES 08 Second Eur. Conf. Mech. Sci.*, 431–438. Springer.